EMP Theoretical Notes

Note 177

ELECTROMAGNETIC PULSE (EMP) PROPAGATION THROUGH AN ABSORPTIVE AND DISPERSIVE MEDIUM

by

D. Arnush

TRW SYSTEMS GROUP
One Space Park, Redondo Beach, CA 90278

30 June 1971

This work supported under
Air Force Contract No. F04(701)-70-C-0165

ELECTROMAGNETIC PULSE (EMP)* PROPAGATION THROUGH AN ABSORPTIVE AND DISPERSIVE MEDIUM

by

D. Arnush

ABSTRACT

A numerical technique for solving the high frequency approximation EMP equations is presented. The Lorentz model of the secondary electron current is used, thereby achieving a result valid for a burst above the ground and observer at any altitude. Comparisons of the results of this technique and those techniques which assume an ohmic secondary electron current are made and it is found that they are identical for observations below 40 km but differ markedly above 80 km.

---

* This work is supported under Air Force Contract No. F04(701)70-C-0165.

Theoretical Physics Group
TRW SYSTEMS GROUP
One Space Park
Redondo Beach, CA 90278

I. INTRODUCTION

In EMP Theoretical Note Number 26[1] (TN26) a numerical technique for solving the high frequency approximation EMP equations was presented. The technique described is appropriate for a geometry in which the source is at a high altitude and the observer at a low altitude, and for a pulse which is sufficiently slowly time-varying to use Ohm's law ($j = \sigma E$) in the time domain. In this report we shall present a more general numerical technique which is appropriate for all those configurations of source and observer for which the high frequency EMP equations are valid and magnetoionic effects may be neglected.

The features of the numerical technique described in TN26 which make it inappropriate for use by a high-altitude observer are: 1) the secondary electron current ($\underline{j}_{sec}$) is assumed to be purely conductive (i.e., Ohm's law is used), and 2) avalanching at high altitudes is neglected. In this note we shall follow Karzas and Latter[2] in employing the Lorentz model to obtain a single expression for $\underline{j}_{sec}$ which is valid at all altitudes. However, in contrast to Karzas and Latter,we shall employ this expression in solving the high frequency EMP equations rather than use the approximation $j = \sigma E$ in the time domain at low altitudes, and neglecting collisions at high altitudes. Townsend's ionization coefficient α will be used to modify the equation for the secondary electron density in such a way as to include the effect of avalanching. A numerical technique, valid at all altitudes of interest, for solving the resulting equations will be formulated in Section II. This method, while decoupling and linearizing the equations in each integration step, ultimately achieves the solution of the coupled nonlinear integrodifferential equations. The results of this method are compared to those of the Ohm's law assumption for some cases of interest in Section III.

II. SOLUTION OF THE PULSE EQUATIONS

Following Karzas and Latter[2] in their use of the high frequency EMP equations, the electric field components are

$$\frac{1}{r}\frac{\partial}{\partial r}(rE_\phi) + \frac{2\pi}{c}(j_{s,\phi} + j_{c,\phi}) = 0 \quad , \tag{1}$$

$$\frac{1}{r}\frac{\partial}{\partial r}(rE_\theta) + \frac{2\pi}{c}(j_{s,\theta} + j_{c,\theta}) = 0 \quad , \tag{2}$$

$$\frac{\partial}{\partial \tau} E_r + 4\pi(j_{s,r} + j_{c,r}) = 0 \quad . \tag{3}$$

The equation for the secondary electron density (n) is

$$\frac{\partial n}{\partial \tau} - \alpha w n = \dot{N}_c \quad , \tag{4}$$

where w is the drift velocity of a secondary electron under the influence of the electric field and α is Townsend's ionization coefficient (the average number per cm of secondary electrons produced by an electron traveling along the electric field). These quantities are functions of the local electric field magnitude E and pressure p. The quantities $\underline{j}_c$ and $\dot{N}_c$ are the Compton current density and Compton induced secondary electron production rate, respectively, and are known functions. In the Lorentz model the secondary electron current density is given by

$$\underline{j}_s(r,\tau) = \int_0^\tau d\tau' \frac{e^2}{m} n(r,\tau')\, \underline{E}(r,\tau') \exp\left[-\int_{\tau'}^{\tau} d\tau'' \nu(r,\tau'')\right] \quad , \tag{5}$$

where $\tau = t - r/c$ is the time at each point r, measured relative to the arrival of the first γ photon at that point. The collision frequency, obtained from the relation

$$\nu = \frac{eE}{mw} \quad , \tag{6}$$

is a function of r and τ through its dependence on E as well as p. Equations (1) to (6) form a set of coupled, nonlinear, integrodifferential equations for $\underline{E}$ and n, subject to the boundary conditions

$$\underline{E}(r,0) = \underline{E}(0,\tau) = 0, \; n(r,0) \text{ prescribed.} \tag{7}$$

We shall solve the equations on the mesh shown in Fig. (1) by integrating them along the line of sight (i.e., along r for fixed τ) to the observation point R for the first, and then each succeeding time increment, $\Delta\tau$. At the given point in the integration shown in Fig. (1) $\underline{E}$ and n are known at points on the mesh with $0 \le r \le R$ for $0 \le \tau \le \tau_1$, and with $0 \le r \le r_1$ for $\tau = \tau_2$. The problem is to obtain $\underline{E}$ and n at the point (r_2,τ_2)(denoted by point 4) given these functions at points 1,2, and 3.

Take the integration mesh sufficiently fine to safely assume that $\underline{j}_c$, $\dot{N}_c$ and p are constant in each integration step. Observing that, for fixed p, ν is a slowly varying function[1] of E, and make the crucial assumption that ν is fixed in each integration step. Now rewrite Eq. (5) as

$$\underline{j}_s(r,\tau) = \underline{j}_s(r,\tau_1)\, e^{-\nu(\tau-\tau_1)} + \int_{\tau_1}^{\tau} d\tau' \, \frac{e^2}{m}\, n(r,\tau')\, \underline{E}(r,\tau')\, e^{-\nu(\tau-\tau')} \quad . \tag{8}$$

Ignoring, for the moment, the distinction between the two transverse components (θ and ϕ), define $G = rE_{\theta,\phi}$, as well as $a = 2\pi e^2 n/(mc) = \omega_p^2/(2c)$ and rewrite Eqs. (1) and (2) as

$$\frac{\partial}{\partial r} G(r,\tau) + \int_{\tau_1}^{\tau} d\tau' \, a\, e^{-\nu(\tau-\tau')}\, G(r,\tau') + \frac{2\pi}{c}\, r\, j_c(r,\tau)$$

$$+ \frac{2\pi}{c}\, r\, j_s(r,\tau_1)\, e^{-\nu(\tau-\tau_1)} = 0 \quad . \tag{9}$$

We have found E_r to be non-negligible only in the immediate neighborhood (within about 1 km) of a low altitude burst. At such locations Ohm's law is appropriate. We shall therefore replace $j_{s,r}$ by σE_r in Eq. (3) where $\sigma = e^2 n/(m\nu)$ (a pedigree for this substitution, based on the Lorentz model, will be presented in Section III). Eq. (3) then becomes

$$\frac{\partial E_r}{\partial \tau} + \frac{4\pi\sigma}{c} E_r + \frac{4\pi}{c}\, j_{c,r}(r,\tau) = 0 \quad . \tag{10}$$

Decouple Eqs. (9) and (10) from (4) assuming some constant value of n to be used in the integration of $\underline{E}$ in the intervals 2-4 and 3-4 (e.g., $\bar{n} = n_2$). Eq. (9) is readily solved by taking its Laplace transform with respect to τ, making use of Eqs. (1) and (2) in eliminating $\underline{j}_s(r,\tau_1)$, and then inverting the transforms. The result is

$$G(r_2,\tau_2) = G(r_1,\tau_1)e^{-z}\, J_0(x) + e^{-z}\int_{\tau_1}^{\tau_2} d\tau'[\nu G(r_1,\tau') + \frac{\partial}{\partial\tau'} G(r_1,\tau')]e^{\nu\tau'} J_0(2\sqrt{a\Delta r(\tau_2-\tau')}$$

$$+ e^{-z}\int_{r_1}^{r_2} dr' \frac{\partial}{\partial r'} G(r',\tau_1)\, J_0(2\sqrt{a\Delta\tau(r_2-r')} \qquad (11)$$

$$- e^{-z}\int_{r_1}^{r_2} dr' \int_{\tau_1}^{\tau_2} d\tau' \frac{2\pi r'}{c}[\nu j_c(r',\tau') + \frac{\partial}{\partial\tau'} j_c(r',\tau')]e^{\nu\tau'} J_0(2\sqrt{a(r_2-r')(\tau_2-\tau')}) \quad ,$$

where

$$\Delta r = r_2-r_1,\ \Delta\tau = \tau_2-\tau_1,\ x = 2\sqrt{a\Delta r\Delta\tau} \text{ and } z = \nu\Delta\tau \quad . \qquad (12)$$

Equation (10) is readily solved with the aid of an integration factor. The result is

$$E_r(r_2,\tau_2) = e^{-y}\left\{E_r(r_2,\tau_1) - \frac{4\pi}{c}\int_{\tau_1}^{\tau_2} d\tau'\, j_{cr}(r_2,\tau')\, e^{\frac{4\pi\sigma}{c}(\tau'-\tau_1)}\right\} \quad , \qquad (13)$$

where $y = 4\pi\sigma\Delta\tau/c$. Equations (11) and (13) give G and E_r at r_2,τ_2 in terms of integrals of these quantities over the intervals 1-2 and 1-3, yet the results of the numerical integrations yield the values of G and E_r only at the points 1, 2, and 3. In order to perform the indicated integrations we shall linearly interpolate the fields in the appropriate intervals; i.e.,

$$G(r_1,\tau') = G_1 + (G_2-G_1)\frac{1}{\Delta\tau}(\tau'-\tau_1) \quad ,$$

$$G(r',\tau_1) = G_1 + (G_3-G_1)\frac{1}{\Delta r}(r'-r_1) \quad , \text{ etc.} \qquad (14)$$

The results are

$$G_4 = [G_1 J_0 + (G_3 - G_1)\, 2J_1/x]e^{-z} + [G_2 F + (G_2 - G_1)\, \frac{\partial}{\partial z} F] \tag{15}$$

$$- \frac{r}{\sigma}\Big\{ j_{c,4}(1 - F) + \frac{1}{z}(j_{c,4} - j_{c,3})(1 - F - z\,\frac{\partial}{\partial z} F) - [j_{c,3} + \frac{1}{z}(j_{c,4} - j_{c,3})]J_0 e^{-z}$$

$$E_{r,4} = E_{r,3}e^{-y} - \frac{1}{\sigma}[(1 - e^{-y})j_{cr,3} + \frac{1}{y}(y - 1 + e^{-y})j_{cr,4}] \quad , \tag{16}$$

where $\sigma = cx^2(8\pi\Delta rz)^{-1} = e^2 n(m\nu)^{-1}$ is the electronic conductivity, J_0 and J_1 are Bessel functions of argument x, and

$$F(x,z) = z\int_0^1 ds\; e^{-zs}\, J_0(x\sqrt{s})$$

$$= e^{-z}\sum_{n=1}^{\infty} (2z/x)^n J_n(x) \tag{17a}$$

$$= \exp\left(-\frac{x^2}{4z}\right) - e^{-z}\sum_{n=0}^{\infty}\left(-\frac{x}{2z}\right)^n J_n(x) \quad , \tag{17b}$$

$$\frac{\partial}{\partial z} F(x,z) = \left(\frac{x}{2z}\right)^2 F + (J_0 - \frac{x}{2z} J_1)e^{-z} \quad . \tag{17c}$$

For the sake of brevity we have simplified Eq. (15) by assuming that j_c is slowly varying in space (i.e., $j_{c,3} = j_{c,1}$ and $j_{c,4} = j_{c,2}$). The two infinite series representations for F shown in Eq. (17) have infinite radii of convergence. Their rates of convergence (and hence their usefulness for numerically calculating F) depend significantly on the value of the ratio 2z/x.

Eq. (4) may be easily solved using a procedure analogous to that used to solve Eq. (3); i.e., assume that αw is slowly varying in a time step. The result is

$$n_4 = n_3 e^u + \frac{1}{\alpha w}[(e^u - 1)\dot{N}_{c,3} + \frac{1}{u}(e^u - 1 - u)\dot{N}_{c,4}] \quad , \tag{18}$$

where $u = \alpha w \Delta\tau$.

III. COMPARISON WITH OHM'S LAW

Eqs. (15), (16), and (18) form the basis for the TRW high altitude EMP computer program CRAIG. As an option, CRAIG has the capability of calculating G from Eqs. (1) and (2) using Ohm's law and a stepwise integration scheme similar to that used in obtaining Eq. (16) from Eq. (3). That is, it uses

$$G_4 = G_2 \exp(-\frac{2\pi\sigma}{c}\Delta r) - \frac{r}{\sigma} j_{c,4}[1 - \exp(-\frac{2\pi\sigma}{c}\Delta r)] \quad . \qquad (19)$$

This result is readily obtainable from Eqs. (15) and (17b, c) by taking the limit $x,z \to \infty$, with $x^2/(4z) = 2\pi\sigma\Delta r/c$. For all cases where the observer is below approximately 40 km, the Lorentz and ohmic solutions of the transverse pulse equations (i.e., Eqs. 15 and 19) yield results which differ by less than 1%. However, at higher altitudes, where the electron collision frequency may become comparable to the rate of change of the field, large deviations may occur.

Consider, for example, a vertical line-of-sight (LOS) above a bomb exploded at an altitude of 20 km. The field value versus altitude at a fixed proper time τ for each altitude is shown in Figure 2. The results of the two models begin to deviate significantly above 80 km. For the soft gamma ray spectrum assumed for these calculations the field generation region lies below 80 km and hence the difference may be attributed to the different propagation mechanisms of the two models. We may note that above this height the Lorentz model of the propagation predicts a highly dispersive character which results in the spatial oscillations shown. Such a behavior could never result from the ohmic model.

Using the same configuration as that described above, Figure 3 contrasts the field values at an altitude of 90 km as a function of time for these two models. The calculation based on the Lorentz model yields a field which both rises and descends more rapidly, and reaches a higher peak. The reason for this behavior may be understood by examining the large ν asymptotic limit for j_s (obtained by an integration by parts in Eq. 5)

$$\underline{j}_s \cong \sigma[\underline{E} - \frac{1}{\nu}\frac{\partial}{\partial t}\underline{E} + \ldots] \quad . \tag{20}$$

The first term in this series represents the Ohm's law approximation. For E increasing ($\dot{E} > 0$) the correction term diminishes the secondary current thereby permitting E to rise faster than the ohmic term would predict. For $\dot{E} < 0$, $\underline{j}_s$ is decreased and E descends less rapidly.

A property of the fields derived from the Lorentz model which has no direct analogue in the ohmic model is that of dispersion. This fact is demonstrated very graphically in Figure 4 where we have considered a bomb exploded at 100 km (where the collision frequency is essentially negligible). The LOS is almost horizontal, so that at the point of observation shown in Figure 4, 500 km away, the altitude is also 100 km. The effect of the intervening plasma has been to take a pulse which would have looked essentially like that shown in Figure 2, filter out its lower frequency fourier components and phase shift the survivors to yield the wavepacket-like shape shown in Figure 4.

ACKNOWLEDGEMENT

The author would like to thank Mr. R.S. Margulies for computer programming the procedures discussed here. He would also like to thank Dr. P. Molmud, as well as Mr. Margulies, for their contributions to many helpful discussions.

REFERENCES

1) Electromagnetic Pulse Theoretical Notes, Volume 2, Number 26, Air Force Weapons Laboratory (WLRE), Kirtland Air Force Base, New Mexico 87117

2) W.J. Karzas and R. Latter, Phys. Rev. 137, B1369 (1965), also Electromagnetic Pulse Theoretical Notes, Volume 2, Number 40, Air Force Weapons Laboratory (WLRE), Kirtland Air Force Base, New Mexico 87117.

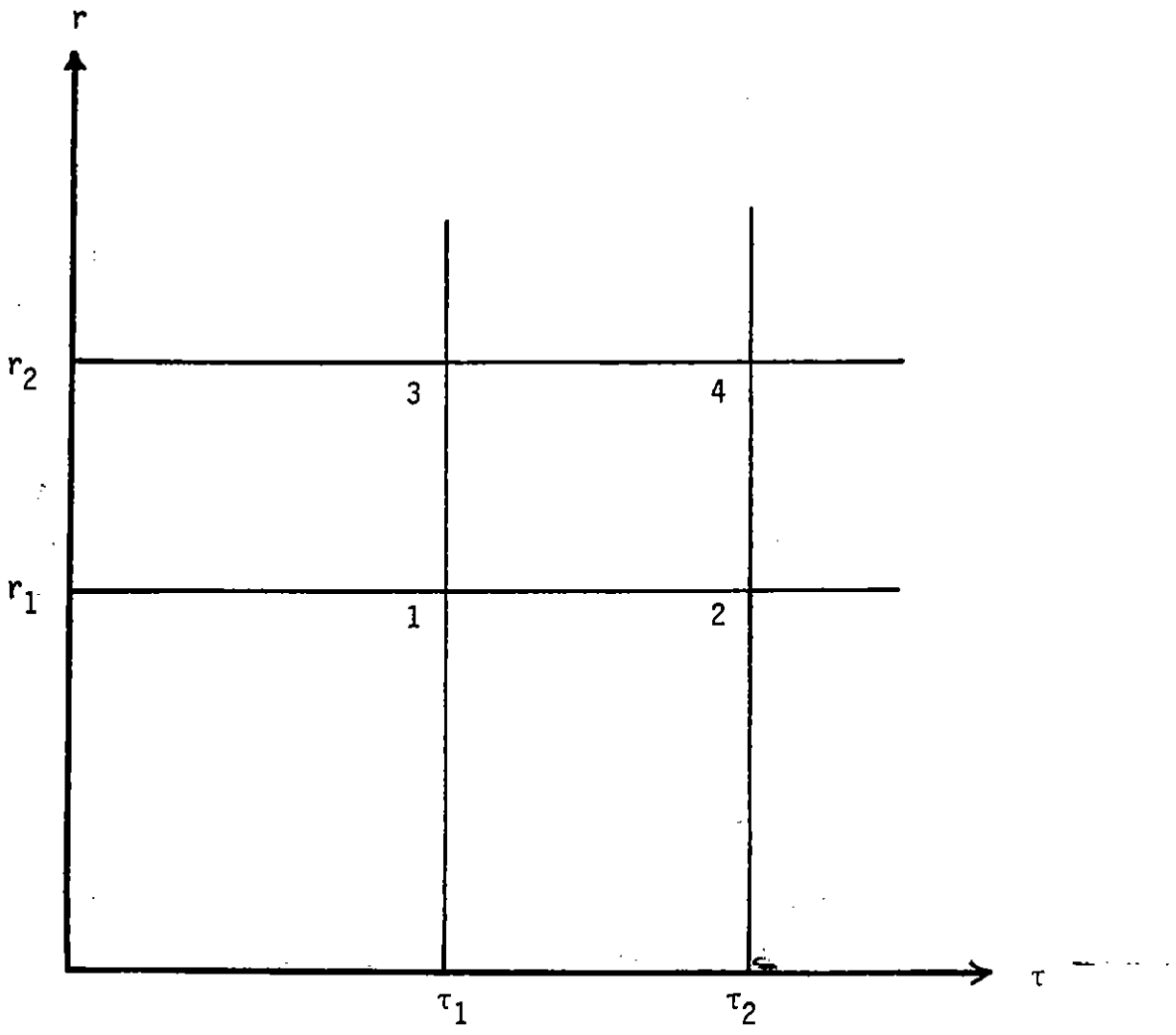

Figure 1 - The integration mesh.

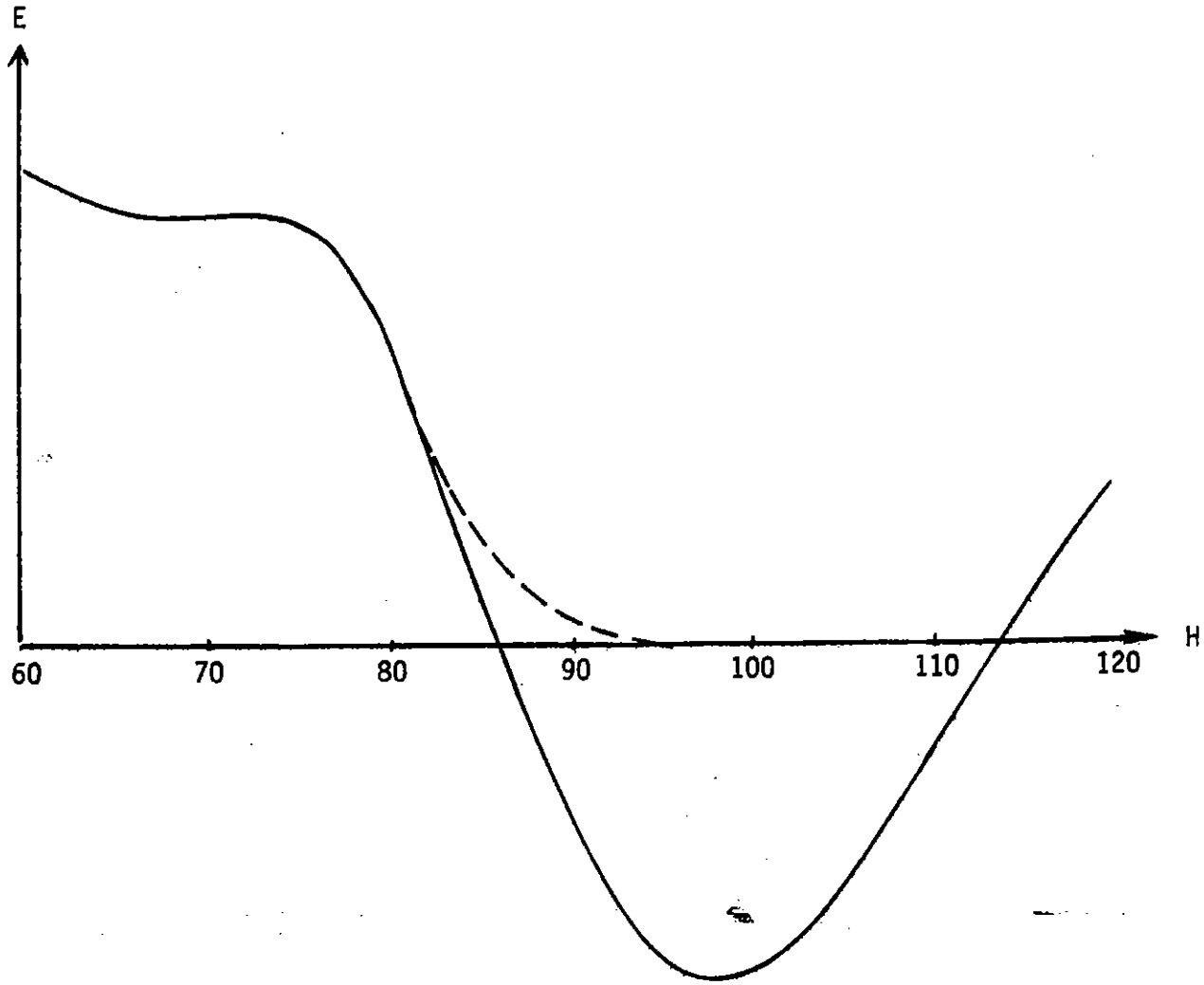

Figure 2 - Electric field (E in arbitrary units) versus altitude (H in km) vertically above a 20 km burst, at a fixed proper time.
——— Lorentz model. — — — Ohm's model.

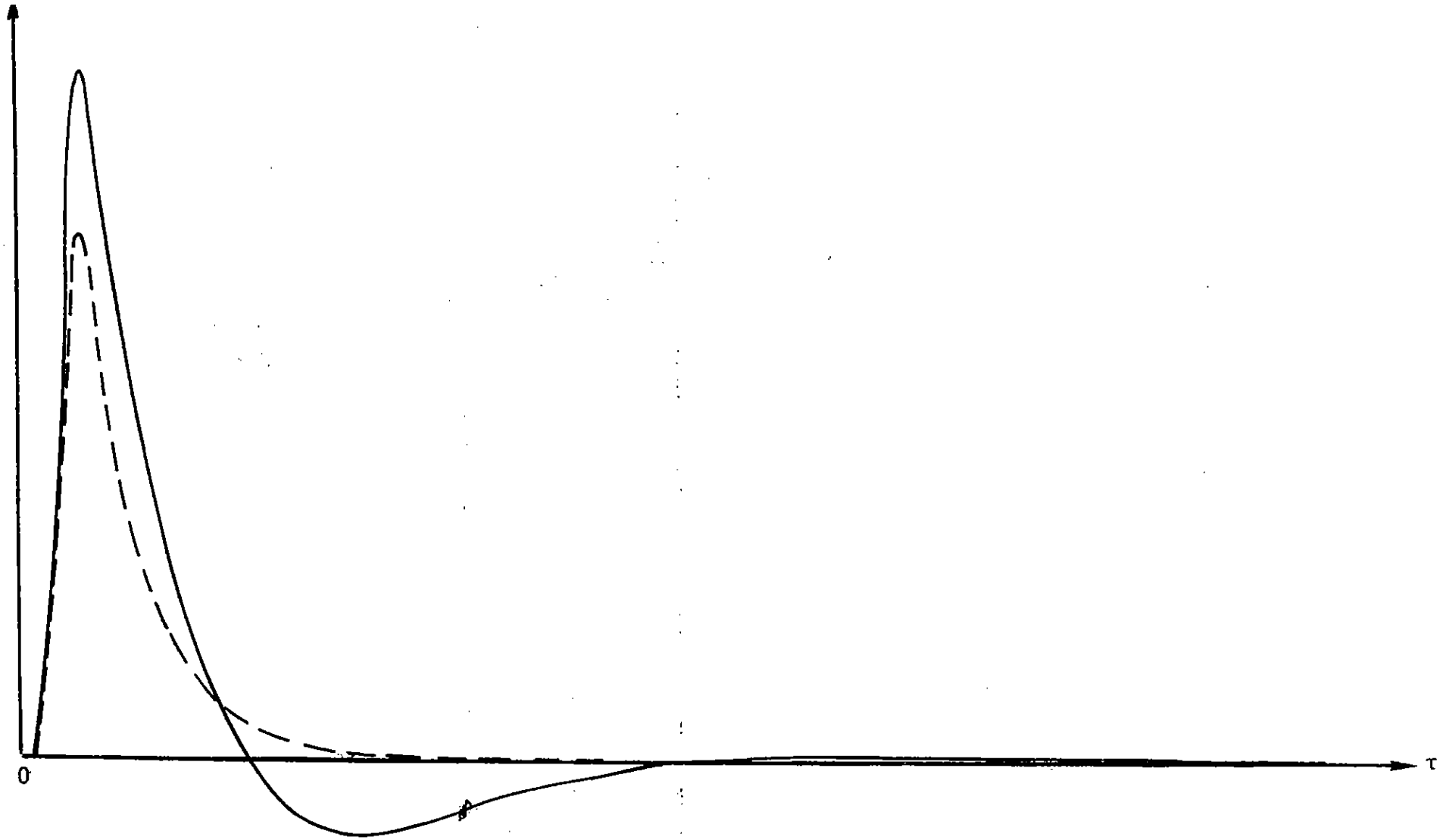

Figure 3 - Electric field (E in arbitrary units) versus proper time (τ in arbitrary units) 90 km above a 20 km burst. ——— Lorentz model. — — — Ohm's model.

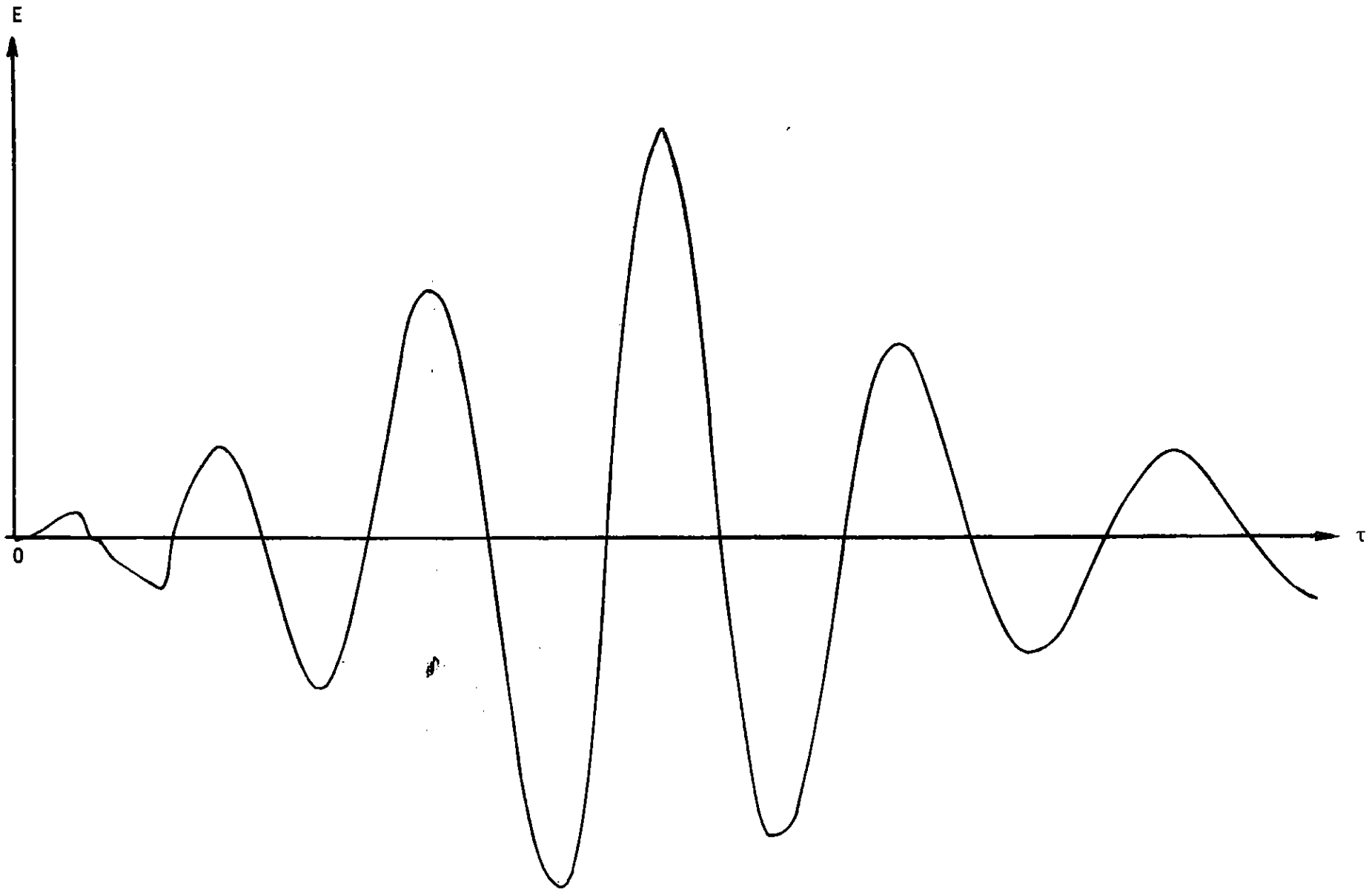

Figure 4 - Electric field (E in arbitrary units) versus proper time (τ, same units as in Figure 3) for bomb and observer at an altitude of 100 km and separated by 500 km.